Part III

Related publications

Paper F

Monotonicity of Control volume methods on triangular grids *

* In Proceedings of the 11th European conference on the mathematics of oil recovery, Sep 8-11th 2008, Bergen,Norway

Monotonicity for control volume methods on unstructured grids

Eirik Keilegavlen[*] [†] [‡], Ivar Aavatsmark[‡]

July 2008

Abstract

In reservoir simulation the pressure is the solution of an elliptic equation. It follows from the maximum principle that this equation satisfies a monotonicity property. This property should be preserved when discretising the pressure equation. If this is not the case, the pressure solution may have false internal oscillations and extrema on no-flow boundaries. Thus, there is a need for sufficient conditions for the discretization methods to be monotone. These conditions will depend on the permeability tensor and the grid.

Previously monotonicity for control volume methods has been studied on quadrilateral grids and on hexagonal grids. The former was done for general methods which reproduces linear potential fields, while the latter was done in a Control Volume Finite Element setting. These analyses have given sharp sufficient conditions for the discretisation methods to be monotone. However, for methods whose cell stencils include cells which do not have any edges common with the central cell in the discretisation scheme, no work has been done on unstructured grids.

In this work, we study monotonicity on triangular grids for control volume methods which are exact for linear potential fields. We derive sufficient conditions for monotonicity of the MPFA-O and -L methods. The found monotonicity regions for the MPFA methods are also tested numerically. The tests are done both on uniform grids in homogeneous media, and on perturbed grids, which corresponds to heterogeneous media. The investigations are done for single phase flow only. However, the results are relevant for multiphase simulations.

The results obtained in this work may be utilised in grid generation. In this way we can construct grids where the discretisation of the pressure equation is guaranteed to be monotone.

1 Introduction

Multiphase flow in an oil reservoir is governed by a set of non-linear partial differential equations. The pressure is the solution of an elliptic equation, while the saturation is described by an almost hyperbolic equation.

It follows from the maximum principle that the elliptic pressure equation satisfies a monotonicity property. This property should be conserved when discretizing the equation. Violations of the monotonicity property might lead to false internal oscillations and extrema on no-flow boundaries. Thus, there is a need for sufficient conditions for the discretization methods to be monotone. These conditions will depend both on the permeability tensor and on the grid.

The hyperbolic behaviour of the saturation calls for numerical methods which are locally conservative. Control volume methods are well suited to discretize the elliptic part of the equations. They are locally conservative, and the explicit flux expression allows for a fully implicit formulation.

[*]Corresponding Author: Eirik.Keilegavlen@cipr.uib.no , Address: CIPR, Allegaten 41, 5007 BERGEN, Norway, Telephone: 0047-55583674

[†]Department of Mathematics, University of Bergen, Bergen, Norway

[‡]Centre for Integrated Petroleum Research, University of Bergen, Bergen, Norway

The geology in the reservoir is characterised by high degrees of heterogeneities and anisotropies. This makes it feasible to use flexible, unstructured grids.

Monotonicity for control volume methods on quadrilateral grids is studied in [3, 11, 9, 10], with special focus on Multipoint Flux Approximation (MPFA) methods. For general quadrilateral grids, sufficient conditions for monotonicity are known. On hexagonal grids, monotonicity has been studied in a Control Volume Finite Element setting. On unstructured grids, we have results for linear methods whose cell stencil includes cells which share an edge with the central cells. These methods, which includes the well known two point flux approximation, are monotone only if they yield a linear system whose matrix is an M-matrix. To our knowledge, no work has been done for more general methods. The focus in this paper is on monotonicity for triangular grids.

2 Monotonicity

We study the elliptic model equation

$$-\mathrm{div}(\mathbf{K}\mathrm{grad}\, u) = q \qquad \mathbf{x} \in \Omega\,, \tag{1}$$

where $\mathbf{K}$ is a symmetric, positive definite tensor and q is a source term. Consider the case where $\mathbf{K}$ is sufficiently smooth and the source is positive, $q \geq 0$. Then u has no minima in Ω. This follows from a version of the maximum principle called Hopf's lemma. Moreover, Hopf's lemma can be stated for any subdomain of Ω. Thus, for a positive source term, u cannot have any local minima in Ω.

The solution of equation (1) with a homogeneous Dirichlet condition, $u = 0\,\mathrm{on}\,\partial\Omega$ can be formulated in terms of a Green's function. We have

$$u(\mathbf{x}) = \int_\Omega G(\boldsymbol{\xi}, \mathbf{x}) q(\boldsymbol{\xi})\, d\tau_{\boldsymbol{\xi}}\,.$$

Here $G(\boldsymbol{\xi}, \mathbf{x})$ is the Green's function for the boundary value problem. For $\mathbf{K}$ and $\partial\Omega$ sufficiently smooth, we have

$$G(\boldsymbol{\xi}, \mathbf{x}) \geq 0 \qquad \boldsymbol{\xi}, \mathbf{x} \in \Omega\,.$$

By Hopf's lemma the Green's function must be positive on any subdomain of Ω. A consequence of this is that for a problem with homogeneous Dirichlet boundary conditions, we have

$$q \geq 0 \Rightarrow u \geq 0\,. \tag{2}$$

A discretization of a differential operator should ideally have the same properties as the continuous operator. The discretization will give a system of linear equations

$$\mathbf{A}\mathbf{u} = \mathbf{q}\,, \tag{3}$$

where $\mathbf{A}$ is the discretized operator, $\mathbf{u}$ and $\mathbf{q}$ is the solution and the source term in each grid block, respectively. The discrete analog of equation (2) is

$$\mathbf{q} \geq 0 \Rightarrow \mathbf{u} \geq 0\,.$$

This is fulfilled if

$$\mathbf{A}^{-1} \geq 0\,, \tag{4}$$

where the inequality holds for all elements in $\mathbf{A}^{-1}$. When the inequality (4) holds, we say that the matrix $\mathbf{A}^{-1}$ is monotone, while $\mathbf{A}$ is inverse monotone. Hopf's lemma can be stated on any subdomain of Ω. Thus the discretisation should yield a matrix whose inverse is monotone not only for the grid covering Ω, but also for all possible subgrids. We call numerical methods which has this property monotone methods.

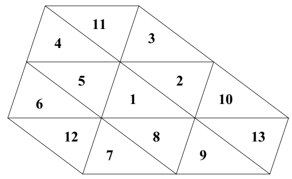

Figure 1: Local ordering of the cell stencil.

A special class of inverse monotone matrices are the M-matrices. These are inverse monotone matrices whose off-diagonal elements are non-positive. Irreducibly diagonally dominant matrices with positive diagonal elements and non-positive off-diagonal elements will be M-matrices. However, this is a sufficient but not necessary criterion for monotonicity.

In [10], the following result was proved: Suppose that the matrix $\mathbf{A}$ has a splitting $\mathbf{A} = \mathbf{B} - \mathbf{C}$, with $\mathbf{B}^{-1} \geq \mathbf{0}$, and $\mathbf{C}\mathbf{B}^{-1} \geq \mathbf{0}$. Suppose further that the inequality

$$\sum_i a_{i,j} \geq 0 \qquad \forall j \,, \tag{5}$$

is either strict for all j, or $\mathbf{C}\mathbf{B}^{-1}$ is irreducible, and (5) is strict for at least one j. Then the inverse of $\mathbf{A}$ is monotone.

We will utilise this result to find sufficient conditions for monotonicity for control volume methods.

3 Monotonicity for 10-point methods on general grids

We now study the monotonicity of control volume methods on triangular grids. Consider the cell stencil shown in figure 1. We firstly focus on methods which express the flux out of cell 1 using all cells in the cell stencil except the cells 11, 12, and 13. We will make a comment on this later. The control volume method approximate the integral of the equation (1) over a cell by

$$\int_{\Omega_{i,j}} q \, d\tau = \int_{\Omega_{i,j}} -\mathrm{div}(\mathbf{K}\mathrm{grad}\, u) \, d\tau \approx \sum_{k=1}^{10} m_k^{(i,j)} u_k \,,$$

where $m_k^{(i,j)}$ are the elements in the cell stencil for cell (i,j) and u_k are the potentials in the cells. By approximating the elliptic equation for all cells in the domain, we obtain a linear system of the form (3).

By applying Hopf's lemma on a subdomain consisting only of the central cell, we find that m_1 must be positive. For subdomains consisting of the central cell and one of the neighbours which shares an edge with this cell (that is, cell number 2, 5, or 8), we need the second cell to have a non-positive coefficient.

To obtain sufficient conditions for the method to be monotone, we utilise the block structure of $\mathbf{A}$. Let $\mathbf{B}$ be the diagonal blocks of $\mathbf{A}$, and denote each of the blocks by $\mathbf{B}_j$. Then $\mathbf{B}_j$ read

$$\mathbf{B}_j = \begin{bmatrix} & \ddots & m_2^{i-1,j} & \ddots & \\ m_6^{i,j} & m_5^{i,j} & m_1^{i,j} & m_2^{i,j} & m_{10}^{i,j} \\ & \ddots & m_5^{i+1,j} & \ddots & \end{bmatrix} .$$

Define $\mathbf{C}$ by $\mathbf{A} = \mathbf{B} - \mathbf{C}$. Then $\mathbf{C}$ consists of the lower and upper diagonal blocks of $\mathbf{A}$, denote these $\mathbf{C}_j^L$ and $\mathbf{C}_j^U$. These matrices read

$$\mathbf{C}_j^L = -\begin{bmatrix} \ddots & m_9^{i-1,j} & \\ m_7^{i,j} & m_8^{i,j} & m_9^{i,j} \\ & m_7^{i+1,j} & \ddots \end{bmatrix}, \qquad \mathbf{C}_j^U = -\begin{bmatrix} \ddots & m_3^{i-1,j} & \\ m_4^{i,j} & 0 & m_3^{i,j} \\ & m_4^{i+1,j} & \ddots \end{bmatrix}.$$

The index i is increasing along the line 6-10, while j is running along the line 7-3, refering to figure 1. Note that the structure of the matrices $\mathbf{C}_j^L$ and $\mathbf{C}_j^U$ will change depending on which cell is the central cell. For cell number $(i+1,j)$, $\mathbf{C}_j^L$ will have a 0 on its diagonal, while the diagonal element of $\mathbf{C}_j^U$ will be nonzero.

To use the results presented in section 2, $\mathbf{B}$ must be monotone. If we require

$$m_1^{i,j} > 0\,, \tag{6}$$
$$\max\{m_2^{i,j}, m_5^{i,j}, m_6^{i,j}, m_{10}^{i,j}\} < 0\,, \tag{7}$$
$$m_1^{i,j} + m_2^{i,j} + m_5^{i,j} + m_6^{i,j} + m_{10}^{i,j} > 0\,, \tag{8}$$

$\mathbf{B}$ will be an M-matrix, and thereby inverse monotone. Define $\mathbf{D} = \mathbf{B}^{-1}$. Next, we consider the positivity of $\mathbf{C}\mathbf{B}^{-1}$. Define the block matrices $\mathbf{D}_j$, $\mathbf{E}_{j+1}^L$, and $\mathbf{E}_{j-1}^U$ by

$$\mathbf{D}_j = \mathbf{B}_j^{-1}\,, \qquad \mathbf{E}_{j+1}^L = \mathbf{C}_{j+1}^L \mathbf{D}_j\,, \qquad \mathbf{E}_{j-1}^U = \mathbf{C}_{j-1}^U \mathbf{D}_j\,.$$

We write the coefficients as

$$\mathbf{D}_j = \{d_{i,k}^j\}\,, \qquad \mathbf{E}_j^L = \{e_{i,k}^{j,L}\}\,, \qquad \mathbf{E}_j^U = \{e_{i,k}^{j,U}\}\,.$$

Because $\mathbf{D}$ is the inverse of $\mathbf{B}$, we have

$$m_6^{i,j} d_{i-2,k}^j + m_5^{i,j} d_{i-1,k}^j + m_1^{i,j} d_{i,k}^j + m_2^{i,j} d_{i+1,k}^j + m_{10}^{i,j} d_{i+2,k}^j = \delta_{i,k}\,,$$

that is

$$d_{i,k} = \frac{\delta_{i,k}}{m_1^{i,j}} - \frac{m_6^{i,j} d_{i-2,k}^j}{m_1^{i,j}} - \frac{m_5^{i,j} d_{i-1,k}^j}{m_1^{i,j}} - \frac{m_2^{i,j} d_{i+1,k}^j}{m_1^{i,j}} - \frac{m_{10}^{i,j} d_{i+2,k}^j}{m_1^{i,j}}\,,$$

which yields

$$\begin{aligned} e_{i,k}^{j+1,L} &= -\left(m_7^{i,j} d_{i-1,k}^j + m_8^{i,j} d_{i,k}^j + m_9^{i,j} d_{i+1,k}^j\right) \\ &= -\frac{\delta_{i,k}}{m_1^{i,j}} m_8^{i,j} + \left(\frac{m_8^{i,j}}{m_1^{i,j}} m_6^{i,j}\right) d_{i-2,k}^j + \left(\frac{m_8^{i,j}}{m_1^{i,j}} m_5^{i,j} - m_7^{i,j}\right) d_{i-1,k}^j \\ &\quad + \left(\frac{m_8^{i,j}}{m_1^{i,j}} m_2^{i,j} - m_9^{i,j}\right) d_{i+1,k}^j + \left(\frac{m_8^{i,j}}{m_1^{i,j}} m_{10}^{i,j}\right) d_{i+2,k}^j\,, \end{aligned}$$

and

$$e_{i,k}^{j+1,U} = -\left(m_4^{i,j} d_{i-1,k}^j + m_3^{i,j} d_{i+1,k}^j\right).$$

Now, $\mathbf{B}$ is an M-matrix, thus all the elements in $\mathbf{D}$ is non-negative. In order to have all the elements in the $\mathbf{E}$-matrices non-negative, we need

$$\max\{m_3^{i,j}, m_4^{i,j}, m_8^{i,j}\} < 0\,, \tag{9}$$
$$\min\{m_8^{i,j} m_5^{i,j} - m_1^{i,j} m_7^{i,j}, m_8^{i,j} m_2^{i,j} - m_1^{i,j} m_9^{i,j}\} > 0\,. \tag{10}$$

Thus, we have obtained requirements for $m_7^{i,j}$ and $m_9^{i,j}$ which are weaker than an M-matrix criterion.

We have used a logically Cartesian ordering of the cells, with the i-index running along the axis from cell 6 to cell 10, referring to figure 1. The j-axis runs from cell 8 to cell 11. There are two other natural orderings of the cell. We can have one axis from cell 4 to cell 9, and the other axis either from cell 6 to cell 9 or from cell 3 to cell 7. All the three orderings will give sufficient conditions for monotonicity of the control volume method. For each ordering two cells have conditions which are weaker than the M-matrix criterion. To obtain as sharp results as possible, the weak conditions should be used for the cells which are of least importance for the potential in the central cell. The influence from one cell on the potential in another cell will be dependent both on the geometry and on the permeability tensor.

We have only considered cell stencils which uses 10 cells to discretise the equation. It would be natural to use all cells which have a common vertex with the central cell, that is, all cells in figure 1. However, the splitting technique for the matrix used above does not work for these expanded cell stencils. The reason is that whatever we do with the global ordering of the cells, we end up with requiring that one of the cells 11, 12, or 13 must give a negative contribution to the system matrix, which is a very strong condition. These are the cells which presumingly are least important for the flow through the central cell. Hence, the conditions for monotonicity of the discretisation method will not be sharp. To study monotonicity for 13 point cell stencils, we need another technique to obtain sufficient conditions for the monotonicity of the method.

4 Monotonicity on a uniform grid in a homogeneous medium

Next we study control volume methods which are exact for linear potentials. We still limit ourselves to methods which have six cells in the flux molecule for each edge, see figure 2(a). This means that the coefficients m_{11}, m_{12}, and m_{13} is zero for all cells. Moreover, we use the barycentre as the centre of the cells. The grid is assumed to be uniform, and the medium homogeneous.

4.1 General methods

The flux over an edge can be written in terms of the potential in the cells in the flux molecule. Using the local cell numbering in figure 1, and edge numbering as in figure 2(b), we get

$$f_1 = t_{1,1}u_1 + t_{1,2}u_2 + t_{1,3}u_3 + t_{1,5}u_6 + t_{1,8}u_8 + t_{1,10}u_{10}\,.$$

where $t_{1,i}$ are called transmissibility coefficients. Due to symmetry, we have

$$t_{1,1} = -t_{1,2}\,, \qquad t_{1,3} = -t_{1,8}\,, \qquad t_{1,5} = -t_{1,10}\,,$$

hence

$$f_1 = t_{1,1}(u_1 - u_2) + t_{1,8}(u_8 - u_3) + t_{1,10}(u_{10} - u_5)\,. \tag{11}$$

Similarly, for the fluxes out of edge number 2 and 3 we get

$$\begin{aligned} f_2 = &\quad t_{2,1}(u_1 - u_5) + t_{2,2}(u_2 - u_6) + t_{2,4}(u_4 - u_8)\,, \\ f_3 = &\quad t_{3,1}(u_1 - u_8) + t_{3,5}(u_5 - u_9) + t_{3,7}(u_7 - u_2)\,. \end{aligned}$$

We define the quantities r, s, and t by

$$r = \frac{1}{V}\mathbf{a}_1^T\mathbf{K}\mathbf{a}_1\,, \qquad s = \frac{1}{V}\mathbf{a}_2^T\mathbf{K}\mathbf{a}_2\,, \qquad t = \frac{1}{V}\mathbf{a}_3^T\mathbf{K}\mathbf{a}_3\,, \tag{12}$$

where $\mathbf{a}_i$ is the normal vector belonging to edge i, with length equal to the length of the edge, see figure 2(b). All the normal vectors are pointing out of the central cell. The area of the cell is denoted by V. With no loss of generality, we also assume that

$$r \geq s \geq t\,. \tag{13}$$

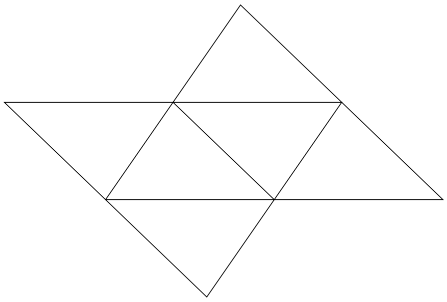

(a)

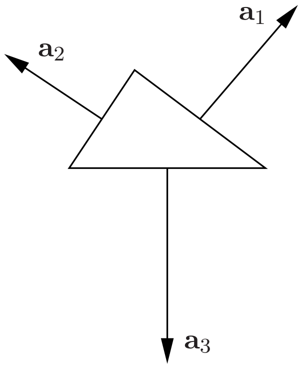

(b) A cell with its normal vectors.

Figure 2: To the left, a flux molecule with six points. To the fight, a cell with its normal vectors.

In each flux expression, there are three transmissibilities. The flux should be exact for linear potential field. For such a field, the gradient can be expressed as

$$\begin{aligned}\nabla u = \;& \tfrac{3}{2V}\Big(\tfrac{1}{3}(2\mathbf{a}_1+\mathbf{a}_2)(u_2-u_1)+\tfrac{1}{3}(\mathbf{a}_1+2\mathbf{a}_2)(u_5-u_1)\Big) \\ = \;& \tfrac{3}{2V}\Big(\tfrac{1}{3}(2\mathbf{a}_2+\mathbf{a}_3)(u_5-u_1)+\tfrac{1}{3}(\mathbf{a}_2+2\mathbf{a}_3)(u_8-u_1)\Big) \quad .\end{aligned} \tag{14}$$

By applying these expressions in two linear independent directions, we remove two degrees of freedom in the flux expressions. First, consider the case where the potential is such that the flux over edge number 1 is zero. Inserting the gradients into $f_1 = -\mathbf{a}_1^T\mathbf{K}\nabla u$, and utilising the relations $\sum_{i=1}^{3}\mathbf{a}_i = \mathbf{0}$ and $\frac{1}{V}\mathbf{a}_1^T\mathbf{K}\mathbf{a}_1 = \frac{1}{2}(-r-s+t)$, we get

$$(u_1-u_2) = \frac{2(s-t)}{3r-s+t}(u_1-u_5)\,, \qquad (u_1-u_8) = -\frac{3r+s-t}{3r-s+t}(u_1-u_5)\,,$$

and equation (11) becomes

$$\Big((s-t)t_{1,1}+t_{1,8}\big(3r+2(s-t)\big)+t_{1,10}\big(3r-2(s-t)\big)\Big)(u_1-u_5)=0\,. \tag{15}$$

where we also have used that for a linear potential field we have

$$(u_8-u_3) = -2(u_1-u_8)+(u_1-u_2)\,, \qquad (u_{10}-u_5) = 2(u_5-u_1)+(u_1-u_2)\,.$$

Next, we let the gradient be parallel to $\mathbf{a}_1$. Then

$$(u_8-u_3) = -(u_{10}-u_5) = 2(u_1-u_2)\,.$$

Equation (11) then becomes

$$f_1 = (t_{1,1}+2t_{1,8}-2t_{1,10})(u_1-u_2) = \frac{r}{2}(u_1-u_2)\,. \tag{16}$$

The equations (15) and (16) can now be combined to give

$$t_{1,1} = \frac{r}{2}+\frac{1}{3}(-s+t)-4t_{1,8}\,, \qquad t_{1,10} = \frac{1}{6}(-s+t)-t_{1,8}\,.$$

Similarly, we get

$$t_{2,1} = \frac{1}{3}(r-t)+\frac{s}{2}-4t_{2,2}\,, \qquad t_{2,2} = \frac{1}{6}(r-t)-t_{2,4}\,,$$

$$t_{3,5} = \frac{1}{12}(-r+s) + \frac{t}{8} - \frac{1}{4}t_{3,1}\,, \qquad t_{3,7} = \frac{1}{12}(-r+s) - \frac{t}{8} + \frac{1}{4}t_{3,1}\,.$$

For the elements in the system matrix, we get

$$\begin{aligned}
m_1 = t_{1,1} + t_{2,1} + t_{3,1} &= \frac{1}{6}(r+s+4t) - 4t_{1,8} + 4t_{2,4} + t_{3,1}\,,\\
m_2 = -t_{1,1} + t_{2,2} - t_{3,7} &= \frac{1}{8}(-2r+2s-3t) + 4t_{1,8} - t_{2,4} - \frac{1}{4}t_{3,1}\,,\\
m_3 &= -t_{1,8}\,, \qquad m_4 = t_{2,4}\,,\\
m_5 = -t_{1,10} - t_{2,1} + t_{3,5} &= \frac{1}{8}(2r-2s-3t) + t_{1,8} - 4t_{2,4} - \frac{1}{4}t_{3,1}\,,\\
m_6 = \frac{1}{6}(r-t) - t_{2,4}\,, \qquad m_7 = t_{3,7} &= \frac{1}{12}(s-r) - \frac{t}{8} + \frac{1}{4}t_{3,1}\,,\\
m_8 = t_{1,8} - t_{2,4} - t_{3,1} &= \frac{1}{6}(-r+t) + t_{1,8} + t_{2,4} - t_{3,1}\,,\\
m_9 = -t_{3,5} = \frac{1}{24}(2r-2s-3t) + \frac{1}{4}t_{3,1}\,, \qquad m_{10} = t_{1,10} &= \frac{1}{6}(-s+t) - t_{1,8}\,,
\end{aligned}$$

Inserting the expressions for m_1 to m_{10} into the above inequalities, we get

$$t_{1,8} > 0\,, \qquad t_{2,4} < 0\,, \qquad t_{3,1} - t_{2,4} - t_{1,8} > \frac{1}{6}(t-r)\,, \tag{17}$$

$$\begin{aligned}
&\Big(\frac{1}{6}(-r+t) + t_{1,8} + t_{2,5} - t_{3,1}\Big)\Big(\frac{1}{8}(2r-2s-3t) + t_{1,8} - 4t_{2,4} - \frac{1}{4}t_{3,1}\Big)\\
&\qquad -\Big(\frac{1}{6}(r+s+4t) - 4t_{1,8} + 4t_{2,4} + t_{3,1}\Big)\Big(\frac{1}{12}(-r+s) - \frac{t}{8} + \frac{1}{4}t_{3,1}\Big) > 0\,,\\
&\Big(\frac{1}{6}(-r+t) + t_{1,8} + t_{2,4} - t_{3,1}\Big)\Big(\frac{1}{8}(-2r+2s-3t) + 4t_{1,8} - t_{2,4} - \frac{1}{4}t_{3,1}\Big)\\
&\qquad -\Big(\frac{1}{6}(r+s+4t) - 4t_{1,8} + 4t_{2,4} + t_{3,1}\Big)\Big(\frac{1}{24}(2r-2s-3t) + \frac{1}{4}t_{3,1}\Big) > 0\,.
\end{aligned}$$

These inequalities are the most general set of conditions for monotonicity of a method with a 6 point flux stencil. A general method whose cell stencil consists of ten cells thus has 3 parameters which defines the method. Allowing flux molecules with 10 cells, corresponding to using all the cells in figure 1 for the cell stencil, will introduce another 6 parameters into the equations. The properties of these extended methods can be explored in the same way as above, but the results will be much more complicated. Even if we obtain expressions for the elements m_i, we have no way to tell if matrices which are not M-matrices still are inverse monotone.

4.2 The MPFA L-method

The L-method was introduced in [3] for quadrilateral grids, and applied on triangular grids in [8]. The flux molecule for the L-method consists of three cells. The method approximates the gradient in a cell by a linear function. This gives us 9 degrees of freedom. Three of these are used for the potential in the cell centres. For each of the two edges in the flux molecule, both the flux and the potential is continuous. The continuity of the potential means that the gradient used in the L-method can be expressed by the potential in the three cell centres in the interaction region. Consider the cells shown in figure 3(a). The L-method compute the fluxes over edge number 1 and 5 by using cell number 1, 2, and 6. The gradient in the interaction region can be expressed by

$$\nabla u = \frac{3}{2V}\Big(\frac{1}{3}(2\mathbf{a}_2 + \mathbf{a}_3)(u_2 - u_1) + \frac{1}{3}(\mathbf{a}_2 + 2\mathbf{a}_3)(u_6 - u_1)\Big)\,,$$

where the vectors $\mathbf{a}_i$ are defined as in figure 2(b). The flux becomes

$$f_1 = -\frac{1}{2}\mathbf{a}_2^T \mathbf{K}\nabla u = \frac{1}{8}\Big((-r-3s+t)(u_2-u_1) + 2(-r+t)(u_6-u_1)\Big)\,, \tag{18}$$

where r, s, and t are defined by (12). We can also use the cells 1, 2, and 3 to compute the flux over edge number 1. This gives us

$$f_1 = \frac{1}{8}\Big((r-3s-t)(u_1-u_2) + 2(r-t)(u_3-u_2)\Big)\,. \tag{19}$$

Thus, we have two sets of transmissibilities, with cell 1 and 2 as the central cell, respectively. Define t_1 as the transmissibility of cell 1, when this cell is the central one, and t_2 in a analogous manner. For quadrilateral grids, the choice was made by comparing the magnitude of the transmissibilities t_1 and t_2 [3]. If $|t_1| < |t_2|$ we use t_1, else use t_2. This criterion, although somewhat ad hoc, leads to a method with a compact cell stencil and nice monotonicity properties. We will use the same criterion on triangular grids. The relationship $r \geq s \geq t$ leads us to use expression (19) for the flux. We proceed in the same manner, and get the flux expressions $\mathbf{f} = \mathbf{T}\mathbf{u}$, where $\mathbf{f} = (f_1, \ldots, f_6)$,

$$\mathbf{T} = \frac{1}{8}\begin{bmatrix} r-3s-t & 3(-r+s+t) & 2(r-t) & 0 & 0 & 0 \\ 0 & 2(-r+s) & 3(r-s-t) & -r+s+3t & 0 & 0 \\ 0 & 0 & 0 & 2(-s+t) & 3(-r+s-t) & 3r-s+t \\ 0 & 0 & 0 & -r+3s+t & 3(r-s-t) & 2(-r+t) \\ r-s-3t & 0 & 0 & 0 & 2(r-s) & 3(-rs+t) \\ 2(s-t) & 3(r-s+t) & -3r+s-t & 0 & 0 & 0 \end{bmatrix}.$$

The flux over the edges in cell 1 then becomes

$$\begin{aligned} f_1 =& (t_{6,2}+t_{3,6})u_1 + (t_{6,3}+t_{3,5})u_2 + t_{6,4}u_3 + t_{6,1}u_5 + t_{3,1}u_8 + t_{3,4}u_{10} \\ =& \frac{1}{4}(3r-2s+2t)(u_1-u_2) + \frac{1}{4}(s-t)(u_5-u_{10})\,, \\ f_2 =& (t_{1,2}+t_{4,4})u_1 + t_{1,3}u_2 + t_{1,6}u_4 + (t_{1,1}+t_{4,5})u_5 + t_{4,6}u_6 + t_{1,3}u_8 \\ =& \frac{1}{4}(3s+2t-2r)(u_1-u_5) + \frac{1}{4}(r-t)(u_2-u_6)\,, \\ f_3 =& (t_{2,4}+t_{5,6})u_1 + t_{5,5}u_2 + t_{2,5}u_5 + t_{2,2}u_7 + (t_{2,3}+t_{5,1})u_8 + t_{5,2}u_9 \\ =& \frac{1}{4}(2s+3t-2r)(u_1-u_8) + \frac{1}{4}(r-s)(u_2-u_7)\,. \end{aligned}$$

We note that none of the cells 3,4, nor 9 contributes to the cell stencil. Thus for a homogeneous medium on a uniform grid the L-method only uses 7 cells to express the potential over the edges.

For the L-method to be monotone, we need $m_5 < 0$, that is

$$2r - 2s - 3t < 0\,, \tag{20}$$

When inserting the expressions for m_i into (6)- (10), it turns out that (20) also gives a sufficient condition for monotonicity. Also, when (20) holds, the system matrix will be an M-matrix. Thus the L-method will yield an M-matrix whenever it is monotone. An analogous result holds for quadrilateral grids.

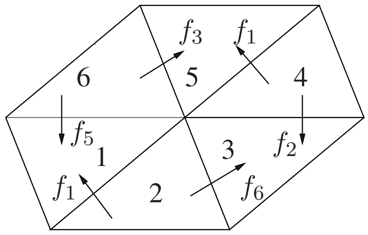

(a)

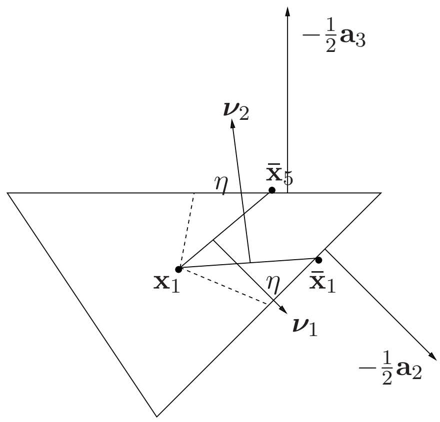

(b)

Figure 3: To the left local ordering of cells and edges, and direction of the fluxes. To the right, vectors used to express the gradient in cell 1, where $\boldsymbol{\nu}_1 = \frac{1}{3}(-\mathbf{a}_2) + \frac{1}{2}(\frac{1}{3} - \eta)(-\mathbf{a}_3)$ and $\boldsymbol{\nu}_2 = \frac{1}{3}(-\mathbf{a}_3) + \frac{1}{2}(\frac{1}{3} - \eta)(-\mathbf{a}_2)$

4.3 The MPFA O(η)-method

The MPFA O-method was studied in [1, 2, 4, 5, 6]. The MPFA O(η)-method expresses the potential in each cell in the interaction region by a linear function. For a uniform triangular grid this leaves in total $3 \cdot 6 = 18$ degrees of freedom. We fix the potential in the cell centre for each cell, using 6 degrees of freedom. We need six degrees of freedom to ensure continuity of the flux for all edges. The potential is continuous only in one point on each edge, as opposed to the L-method, which has full continuity of the potential. As we will see, this makes the flux expressions for the O-method much more complicated.

We denote the cell centre potential in cell i by u_i. Define the continuity point on an edge by

$$\bar{\mathbf{x}}_j = \eta \mathbf{x}_0 + (1 - \eta)\mathbf{x}_{mp}\,, \tag{21}$$

where $\mathbf{x}_{mp}$ is the midpoint of the edge, and $\mathbf{x}_0$ is the vertex lying in the centre of the interaction region. The potential in $\bar{\mathbf{x}}_j$ is denoted $\bar{u}_j$. Consider the interaction region shown in figure 3(a). Using the potentials $u_1, \bar{u}_1$, and $\bar{u}_5$, the gradient in cell 1 can be written as

$$\nabla u^{(1)} = \frac{18}{(4 - (3\eta - 1)^2)V}\Big(\big(\frac{1}{3}(-\mathbf{a}_2) + \frac{1}{2}(\frac{1}{3} - \eta)(-\mathbf{a}_3)\big)(\bar{u}_1 - u_1) \tag{22}$$

$$+ \big(\frac{1}{3}(-\mathbf{a}_3) + \frac{1}{2}(\frac{1}{3} - \eta)(-\mathbf{a}_2)\big)(\bar{u}_5 - u_1)\Big)\,, \tag{23}$$

where V is the area of the cell, and the vectors $\mathbf{a}_i$ are orthogonal on the edges of the triangle as shown in figure 3(a). The length of $\mathbf{a}_i$ is equal to the length of the edge they are orthogonal to, see figure 2(b). By using this expression, we get for the flux over edge 1

$$f_1 = -\frac{1}{2}\mathbf{a}_2^T \mathbf{K} \nabla u^{(1)} = \frac{9}{2(4 - (3\eta - 1)^2)}\Big(\big(\frac{1}{12}(r + 3s - t) + \frac{\eta}{4}(-r + s + t)\big)(\bar{u}_1 - u_1)$$
$$+ \big(\frac{1}{6}(r - t) - \frac{\eta}{2}s\big)(\bar{u}_6 - u_1)\Big)\,,$$

where r, s, and t are defined in equation (12). The gradients in the other cells can be expressed in a similar way. By requiring continuity of the flux, we get a linear system of equations $\mathbf{A}\mathbf{v} = \mathbf{B}\mathbf{u}$, where $\mathbf{v} = (\bar{u}_1, \ldots, \bar{u}_6)$ and $\mathbf{u} = (u_1, \ldots, u_6)$. Note that we have here implicitly have required equality of the potentials on the edges. If we define

$$\mathbf{E} = \frac{1}{2}\mathrm{diag}\Big(- s(1+\eta), -t(1+\eta), -r(1+\eta)\Big) ,$$

and

$$\mathbf{F} = \frac{1}{6}\begin{bmatrix} 0 & -r+t+3s\eta & r-t+3s\eta \\ -r+s+3t\eta & 0 & r-s+3t\eta \\ s-t+3r\eta & -s+t+3r\eta & 0 \end{bmatrix} ,$$

we can write

$$\mathbf{A} = \begin{bmatrix} \mathbf{E} & \mathbf{F} \\ -\mathbf{E} & -\mathbf{F} \end{bmatrix} ,$$

while $\mathbf{B}$ reads

$$\mathbf{B} = \frac{1-\eta}{4}\begin{bmatrix} -r-s+t & r-s-t & 0 & 0 & 0 & 0 \\ 0 & 0 & r-s-t & -r+s-t & 0 & 0 \\ 0 & 0 & 0 & 0 & -r+s-t & -r-s+t \\ 0 & 0 & 0 & r+s-t & -r+s+t & 0 \\ r-s+t & 0 & 0 & 0 & 0 & -r+s+t \\ 0 & r-s+t & r+s-t & 0 & 0 & 0 \end{bmatrix} .$$

The linear system can be solved to obtain $\mathbf{v} = \mathbf{A}^{-1}\mathbf{B}\mathbf{u}$. The flux over the edges can be written as $\mathbf{f} = \mathbf{C}\mathbf{v} + \mathbf{D}\mathbf{u}$. We let

$$\begin{aligned}\mathbf{G} = \frac{1}{12}\mathrm{diag}\Big((r+3s-t) + 3\eta(-r+s+t), (-r+s+3t) + 3\eta(r-s+t), \\ (3r-s+t) + 3\eta(r+s-t)\Big) ,\end{aligned}$$

and

$$\mathbf{H} = \frac{1}{6}\begin{bmatrix} 0 & (r-t)-3s\eta & 0 \\ 0 & 0 & (s-r)-3t\eta \\ (t-s)-3r\eta & 0 & 0 \end{bmatrix} ,$$

and write

$$\mathbf{C} = \frac{9}{2(4-(1-3\eta)^2)}\begin{bmatrix} \mathbf{G} & \mathbf{H} \\ -\mathbf{G} & -\mathbf{H} \end{bmatrix} ,$$

while

$$\mathbf{D} = \frac{9(1-\eta)}{8(4-(1-3\eta)^2)}\begin{bmatrix} -r-s+t & 0 & 0 & 0 & 0 & 0 \\ 0 & 0 & r-s-t & 0 & 0 & 0 \\ 0 & 0 & 0 & 0 & -r+s-t & 0 \\ 0 & 0 & 0 & r+s-t & 0 & 0 \\ 0 & 0 & 0 & 0 & 0 & -r+s+t \\ 0 & r-s+t & 0 & 0 & 0 & 0 \end{bmatrix} .$$

Inserting the expression for $\mathbf{v}$, we obtain a flux expression $\mathbf{f} = (\mathbf{C}\mathbf{A}^{-1}\mathbf{B} + \mathbf{D})\mathbf{u} = \mathbf{T}\mathbf{u}$. The matrix $\mathbf{T}$ can be computed from the expressions above. However, the elements in the matrix are quite complicated, so we do not give the expressions here.

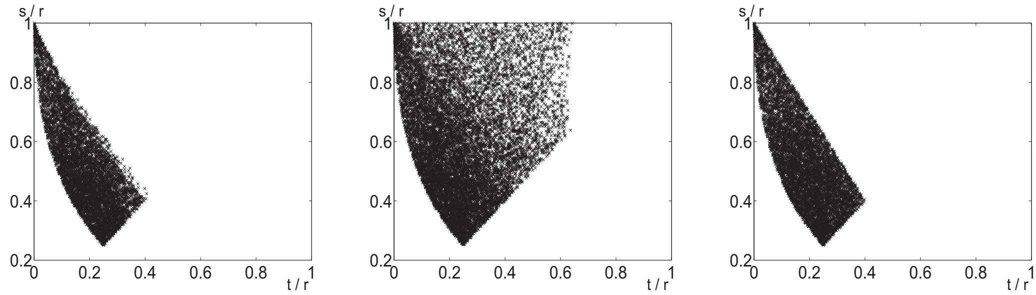

(a) MPFA O(1/3) (b) MPFA O(0) (c) MPFA L

Figure 4: Parameter combinations where the MPFA methods are not monotone. The tests are performed on an unperturbed grid.

Now, consider the cell stencil shown in figure 1. The fluxes over the edges can be expressed as

$$
\begin{aligned}
f_1 =& (t_{6,2} + t_{3,6})u_1 + (t_{6,3} + t_{3,5})u_2 + t_{6,4}u_3 + t_{6,5}u_{11} + t_{6,6}u_4 + t_{6,1}u_5 \\
&+ t_{3,1}u_8 + t_{3,2}u_9 + t_{3,3}u_{13} + t_{3,4}u_{10}\,, \\
f_2 =& (t_{1,2} + t_{4,4})u_1 + t_{1,3}u_2 + t_{1,4}u_3 + t_{1,5}u_{11} + t_{1,6}u_4 + (t_{1,1} + t_{4,5})u_5 \\
&+ t_{4,6}u_6 + t_{4,1}u_{12} + t_{4,2}u_7 + t_{4,3}u_8\,, \\
f_3 =& (t_{5,6} + t_{2,4})u_1 + t_{5,5}u_2 + t_{2,5}u_5 + t_{2,6}u_6 + t_{2,1}u_{12} + t_{2,2}u_7 \\
&+ (t_{2,3} + t_{5,1})u_8 + t_{5,2}u_9 + t_{5,3}u_{13} + t_{5,4}u_{10}\,,
\end{aligned}
$$

where $t_{i,j}$ refers to element (i, j) in the matrix $\mathbf{T}$. If we collect the factors in front of the potentials u_i, we get the elements in the system matrix m_i. These coefficients are rather complicated for a general continuity point η. We will therefore focus on two choices for the parameter η.

For quadrilateral grids, much work has been done on the O(0)-method. Setting $\eta = 0$ gives us $m_{11} = \frac{(r-s)^2}{8(r+s+t)}$ and $m_{12} = \frac{(s-t)^2}{8(r+s+t)}$. With (13) in mind, we conclude that the O(0)-method is never an M-matrix unless $r = s = t$, that is, the grid is K-orthogonal.

In [6], it was shown that the O$(1/3)$-method will always yield a symmetric system matrix on triangular grids. For this choice of η the M-matrix region will be described by the equation $s + t - r > 0$.

The results for the MPFA O-method is not as satisfactory as for the L-method. The reason is that although we can find the transmissibilities, we have no general framework to obtain sharp necessary conditions for monotonicity, due to the limitations mentioned in the end of section 3. The best we can do is to find regions where the method yields an M-matrix.

5 Numerical results

The monotonicity properties of the methods is tested on a grid constructed by dividing a 12 x 12 parallelograms in two, yielding equilateral triangles. The results are visualised by plotting the quantities $\frac{t}{r}$ and $\frac{s}{r}$. Due to (12) and (13) we have

$$0 \le \frac{t}{r} \le \frac{s}{r} \le 1\,,$$

while the requirement that $\mathbf{K}$ is positive definite gives us

$$\left(1 - \sqrt{\frac{t}{r}}\right)^2 \le \frac{s}{r}\,.$$

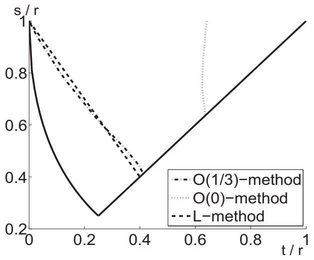

(a) Monotonicity regions for an unperturbed grid.

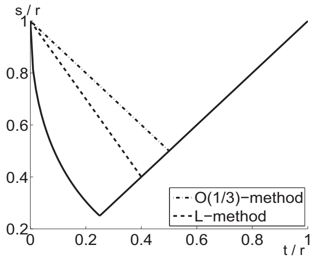

(b) M-matrix regions for an unperturbed grid.

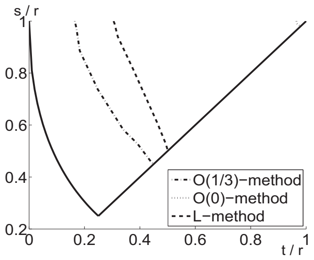

(c) Monotonicity regions for a perturbed grid.

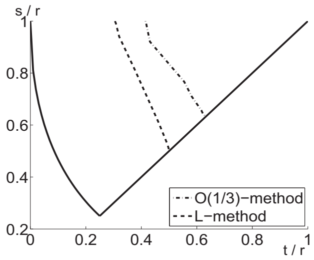

(d) M-matrix regions for a perturbed grid.

Figure 5: Monotonicity and M-matrix regions for both an unperturbed grid and a perturbed grid. The region of ellipticity is to the right of the curved line $\frac{s}{r} = \left(1 - \sqrt{\frac{t}{r}}\right)^2$. The methods are monotone to the right of their respective lines.

We test the monotonicity of the methods in media with random elements in the permeability tensor. The ellipticity of the equation is ensured. The results of such a test is shown in figure 4, and the corresponding regions of monotonicity are plotted in figure 5(a). Figure 5(b) shows the regions where the matrix yields an M-matrix.

For more realistic test cases, we perturb the nodes according to

$$x_{\text{new}} = x_{\text{old}} + \alpha\, r_x \qquad y_{\text{new}} = y_{\text{old}} + \alpha\, r_y\,,$$

where x_{old} and x_{new} are the x-coordinate before and after perturbation, y_{old} and y_{new} are defined similarly, and r_x and r_y are random numbers in the interval $[-0.5, 0.5]$. The monotonicity and M-matrix regions obtained by using $\alpha = 0.2$ are shown in figure 5(c) and 5(d), respectively. The parameters r, s, and t are computed for the grid before the nodes are perturbed. We notice that also for a perturbed grid, the L-method yields an M-matrix whenever it is monotone.

6 Conclusions

In this paper, we have investigated MPFA method on triangular grids, with focus on their monotonicity properties. We have derived expressions for transmissibilities of the L- and the O(η)-method on a uniform grid in a homogeneous medium. These expressions were used to analyse the monotonicity regions of the methods. The analyses of the O-methods are somewhat unsatisfactory due to limitations in our analysis techniques. This should be a topic for further work.

The results obtained in this paper should be considered used to create grids where the MPFA methods are guaranteed to give monotone discretizations. Methods to improve the monotonicity properties of MPFA methods based on the M-matrix property was considered in [7]. With the new results obtained here, it might be possible to extend this work.

References

[1] I. Aavatsmark, T. Barkve, Ø. Bøe, and T. Mannseth. Discretization on unstructured grids for inhomogeneous, anisotropic media. I. Derivation of the methods. *SIAM J. Sci. Comput.*, 19(5):1700–1716, 1998.

[2] I. Aavatsmark, T. Barkve, Ø. Bøe, and T. Mannseth. Discretization on unstructured grids for inhomogeneous, anisotropic media. II. Discussion and numerical results. *SIAM J. Sci. Comput.*, 19(5):1717–1736, 1998.

[3] I. Aavatsmark, G. T. Eigestad, B. Mallison, and J. M. Nordbotten. A compact multipoint flux approximation method with improved robustness. *Numer. Methods Partial Differ. Equations*, 24(5):1329–1360, 2008.

[4] M. G. Edwards. Unstructured, control-volume distributed, full-tensor finite-volume schemes with flow based grids. *Comput. Geosci.*, 6(3-4):433–452, 2002.

[5] M. G. Edwards and C. F. Rogers. Finite volume discretization with imposed flux continuity for the general tensor pressure equation. *Comput. Geosci.*, 2(4):259–290, 1998.

[6] R. A. Klausen, F. Radu, and G. Eigestad. Convergence of mpfa on triangulations and for Richards' equation. *Int. J. Numer. Methods Fluids*, 58(9):1327 – 1351, 2008.

[7] M. Mlacnik and L. Durlofsky. Unstructured grid optimization for improved monotonicity of discrete solutions of elliptic equations with highly anisotropic coefficients. *J. Comput. Phys.*, 216(1):337–361, 2006.

[8] S. Mundal, D. DiPietro, and I. Aavatsmark. Compact-stencil mpfa methods for heterogeneous highly anisotropic second-order elliptic problems. In R. Eymard and J.-M. Herard, editors, *Finite Volumes for Complex Applications V*, pages 905–918. Wiley, 2008.

[9] J. M. Nordbotten and I. Aavatsmark. Monotonicity conditions for control volume methods on uniform parallelogram grids in homogeneous media. *Comput. Geosci.*, 9(1):61–72, 2005.

[10] J. M. Nordbotten, I. Aavatsmark, and G. T. Eigestad. Monotonicity of control volume methods. *Numer. Math.*, 106(2):255–288, 2007.

[11] J. M. Nordbotten and G. T. Eigestad. Discretization on quadrilateral grids with improved monotonicity properties. *J. Comput. Phys.*, 203(2):744–760, 2005.